Molecular Neurobiology (2019) 56:525–534
https://doi.org/10.1007/s12035-018-1080-2

Control of Neuronal Ryanodine Receptor-Mediated Calcium Signaling by Calsenilin

Michael A. Grillo[1] · Stephanie L. Grillo[1] · Bryan C. Gerdes[1] · Jacob G. Kraus[1] · Peter Koulen[1,2]

Received: 16 February 2018 / Accepted: 10 April 2018 / Published online: 5 May 2018

Abstract

Calsenilin is a calcium ion (Ca^{2+})-binding protein involved in regulating the intracellular concentration of Ca^{2+}, a second messenger that controls multiple cellular signaling pathways. The ryanodine receptor (RyR) amplifies Ca^{2+} signals entering the cytoplasm by releasing Ca^{2+} from endoplasmic reticulum (ER) stores, a process termed calcium-induced calcium release (CICR). Here, we describe a novel mechanism, in which calsenilin controls the activity of neuronal RyRs. We show calsenilin co-localized with RyR2 and 3 in the ER of mouse hippocampal and cortical neurons using immunocytochemistry. The underlying protein-protein interaction between calsenilin and the RyR was determined in mouse central nervous system (CNS) neurons using immunoprecipitation studies. The functional relevance of this interaction was assayed with single-channel electrophysiology. At low physiological Ca^{2+} concentrations, calsenilin binding to the cytoplasmic face of neuronal RyRs decreased the RyR's open probability, while calsenilin increased the open probability at high physiological Ca^{2+} concentrations. This novel molecular mechanism was studied further at the cellular level, where faster release kinetics of caffeine-induced Ca^{2+} release were measured in SH-SY5Y neuroblastoma cells overexpressing calsenilin. The interaction between calsenilin and neuronal RyRs reveals a new regulatory mechanism and possibly a novel pharmacological target for the control of Ca^{2+} release from intracellular stores.

Keywords Alzheimer's disease · Calcium · Calsenilin · Cortex · Hippocampus · Ryanodine receptor · RyR

Introduction

Calcium plays an important role in numerous cell signaling pathways in neuronal cells, some of which include memory consolidation, vesicle release, and apoptosis. Due to the ubiquitous nature of intracellular calcium, vital key pathways are employed to convert subcellularly localized alterations in calcium concentrations into global cellular responses [1]. Propagation of intracellular calcium signals throughout the cell is accomplished through calcium release channels such as ryanodine receptors (RyRs) located on intracellular calcium sources, most notably the endoplasmic reticulum [2]. Calcium-binding proteins communicate changes in calcium levels through conformational changes that effect phosphorylation, protein binding, and the action of target proteins [3]. The neuronal calcium sensor family of proteins provide high affinity calcium-binding sites that alter neuronal cell signaling affecting a diverse range of processes, such as memory formation, vesicle release, and neurite outgrowth [4]. In addition, a range of proteins mediate uptake of Ca^{2+} into intracellular stores and extrusion of Ca^{2+} into the extracellular space, which shapes cytoplasmic calcium signaling. These two intimately connected processes, calcium release and calcium sequestration, work synergistically to shape calcium signaling throughout the cell.

RyRs are major calcium-induced calcium release (CICR) channels located on the endoplasmic reticulum membrane in neurons and most other cell types [5]. RyRs are found throughout the nervous system [2, 6, 7] and control multiple processes in neurons through CICR including vesicle release, membrane depolarization, and apoptosis [1]. RyRs contain a large N-terminal cytoplasmic domain, which interacts with proteins, small molecules, and signaling molecules modulating CICR mediated by this channel [3, 8]. Of the three RyRs, RyR1 was originally described in skeletal muscle, RyR2 in

✉ Peter Koulen
koulenp@umkc.edu

[1] Vision Research Center, Department of Ophthalmology, School of Medicine, University of Missouri-Kansas City, Kansas City, MO 64108, USA

[2] Department of Biomedical Sciences, School of Medicine, University of Missouri-Kansas City, Kansas City, MO, USA

heart tissue, and RyR3 in brain tissue, while all three are differentially expressed in most cell types and tissues [1–3]. The three types of RyRs differ in their dependence on the cytosolic Ca^{2+} concentration for activation and inhibition, which, combined with their differential distribution, results in tissue-specific calcium release producing cell- and tissue-specific functions [2]. Previous studies have identified protein-protein interactions between RyRs and cytoplasmic proteins resulting in a change in RyR ion channel activity and Ca^{2+} release from the ER [9, 10]. At the same time, in both in vitro and in vivo disease models of Alzheimer's disease (AD), increased release of Ca^{2+} from ryanodine-sensitive stores was observed in diseased cells [11–14], leading to increased apoptosis of neuronal cells [15, 16]. Similarly, inhibitory control of RyR activity reduced cell damage and cell death in in vitro models of Parkinson's disease [17] and multiple sclerosis [18] and in in vivo models of neuroinflammation [19] and Huntington's disease [20] resulting in reduced functional impairment [19, 20].

Here, we investigated the interactions between calsenilin, a calcium-binding protein also known as KChIP3/DREAM, and RyRs, specifically RyR2 and 3 and determined the impact of this interaction on calcium signaling. Calsenilin is a 31-kDa protein of the neuronal Ca^{2+} sensor family [21] with four C-terminus EF-hand motifs and a unique N-terminus that is responsible for binding to target molecules [22–24]. Calsenilin is found in the human brain [25] and is expressed throughout the CNS, with particularly high expression levels in layers V and VI of the cerebral cortex as well as in the granule layers of the cerebellum, olfactory centers, and the hippocampus [26–30], and it is involved in synaptic plasticity [31–33]. Calsenilin has also been identified in dorsal root ganglia lacking Kv4.3 expression [34], Aβ mechanoreceptors, Aσ sensory receptors, and some C-fiber peptidergic nociceptors [34] of the spinal cord.

Calsenilin interacts with the C-terminus of presenilin 1 and presenilin 2 to stabilize the proteolytic fragments of both presenilin 1 and presenilin 2 [23] and enhance the enzyme activity of the presenilin-γ-secretase complex [35]. Calsenilin alters cellular Ca^{2+} dynamics through several mechanisms, such as controlling the gating kinetics of $Kv_{4.2}$ potassium channels [22], interacting with the downstream regulatory element (DRE) sequence and modulating the transcription of the Na^{+}/Ca^{2+} exchanger NCX3 [24, 36], reversing presenilin 1-mediated enhancement of Ca^{2+} release [37], altering the Ca^{2+} concentration of endoplasmic reticulum stores [36, 38, 39], and increasing Ca^{2+}-induced apoptosis in both cellular and mouse models of AD [40, 41].

Here, we propose that calsenilin acts as a regulator of RyR-mediated CICR that could be used as a potential drug target for controlling calcium dysregulation in neurodegenerative diseases such as AD. Our study shows that calsenilin and brain RyRs, neuronal RyR2 and RyR3, co-localize and interact directly, which results in altered RyR-mediated Ca^{2+} release at the single-channel level. Our functional data from electrophysiology and calcium imaging experiments show that calsenilin alters the Ca^{2+} release kinetics of RyRs at the single-channel level in isolated microsomes and of RyR-channel populations in neuroblastoma cells overexpressing calsenilin. Taken together, these results suggest a novel mechanism whereby calsenilin controls RyR2- and RyR3-mediated CICR release in neurons through direct protein-protein interaction.

Materials and Methods

Immunocytochemistry

NeuroPure™ embryonic day 18 (E18) Sprague Dawley rat cortical cells were prepared following manufacturer's protocol (cat. #N200200, Genlantis, San Diego, CA). Immunostaining was conducted as described previously [42, 43]. Briefly, media was removed and attached cells were fixed for 20 min in 4% PFA (0.01 M PBS, pH 7.4) at room temperature (RT). The fixative was removed, followed by three 10 min washes using PBS (0.01 M PBS, pH 7.4). Blocking solution (10% normal donkey serum, 1% BSA, and 0.05% Triton-X 100 in 0.01 M PBS) was added and cells were incubated for 1 h at RT. After blocking, the cells were incubated with the primary antibodies: DREAM (1:50; sc-9309, Santa Cruz Biotechnologies, Dallas, TX), RyR2 (1:10,000; AB9080, Chemicon Biotechnologies, Temecula, CA), RyR3 (AB9082 (1:5000; Chemicon Biotechnologies) in incubation buffer (3% normal donkey serum, 1% BSA, and 0.05% Triton-X 100 in 0.01 M PBS) overnight at 4 °C. Following primary incubation, cells were washed three times for 10 min with PBS. Cells were next incubated with secondary antibodies: AlexaFluor 488 (1:2000; A11055, Life Technologies, Carlsbad, CA) and AlexaFluor 594 (1:2000; A11062, Life Technologies) and DAPI (1:20,000) for 1 h at RT. After three washes, coverslips were mounted on slides using Aqua-Polymount (Polysciences, Warrington, PA). Negative controls consisted of the omission of the primary antibody.

Preparation of Mouse Brain Sections

C57BL/6 mice (Jackson Laboratories, Bar Harbor, MA) were euthanized using the IACUC approved method of carbon dioxide overdose. Brains were removed from the cranial cavity and immersion fixed in 4% PFA at 4 °C overnight. The tissue was then sequentially cryoprotected in a graded series of 10, 20, and 30% sucrose at 4 °C in PBS. Tissue was removed from final sucrose solution and placed in Peel-A-Way® mold (R-30, Polysciences Inc., Warrington, PA) and incubated at the Tissue-Tek optimal cutting temperature (OCT) embedding medium (Tissue-Tek, Torrance, CA) for 1 h at 4 °C. The samples were then placed in − 80 °C isopentane (Alfa Aesar,

Ward Hill, MA) to solidify the OCT compound and snap-freeze the tissue. Molds were sectioned at 30 μm using a Leica model CM3050 S cryostat.

Immunohistochemistry

Immunohistochemistry was performed as stated previously in the immunocytochemistry section with the addition of the following steps. Before blocking, tissue was placed in 1 mg/ml sodium borohydride (Sigma Aldrich) three times for 10 min [44]. After secondary antibody incubation and subsequent washes, brain sections were incubated in 25 mM $CuSO_4$ for 10 min. The sections were subsequently washed three times with PBS for 10 min, followed by a 10-min wash in deionized water. Coverslips were applied using Aqua-Polymount.

Confocal Microscopy

All immunostaining and colocalization images were acquired on a Leica SP5 white-light laser scanning confocal microscope (Leica Microsystems, Bannockburn, IL) with a 63x glycerin-immersion objective. Alexa 488 was excited at 490 nm and collected at 505–550 nm. Alexa 594 was excited at 594 nm and collected at 599–650 nm. Immunocytochemistry optical sections (z-stack with 0.13 μm z-step, 1.6 optical slice thickness) and immunohistochemistry optical sections (z-stack with 0.13 μm z-step 1.0 optical slice thickness) were collected (2048 × 2048 pixel images) running Leica Application Suite Advanced Fluorescence v 2.6. To ensure uniformity of labeling, all images were acquired with same the confocal settings (pinhole size, gain, offset, and laser power). To decrease signal bleed through, images were collected in the order of Alexa 488, Alexa 594, and DAPI.

Statistical Analysis of Colocalization

Colocalization and intensity analysis were conducted with MBF ImageJ (McMaster Biophotonics Facility, Hamilton, ON) utilizing Pearson's and Mander's coefficient [45]. Pearson's coefficient and Mander's coefficients were validated using the Costes method plugin for Fiji ImageJ.

Recombinant Protein

Glutathione S-transferase (GST)-tagged calsenilin protein was made by transforming bacteria, strain BL21(DE3) pLysS (Novagen, Madison, WI) with a cDNA construct of the full length mouse calsenilin, as described previously [9]. Briefly, calsenilin protein expression was induced by 100 μM IPTG (isopropyl β-$_D$-1-thiogalactopyranoside) at 28 °C for 4 h. Bacterial cultures were then pelleted, lysed, and centrifuged at 18,000×*g* at 4 °C for 20 min. Bacterial protein was extracted by incubation in 50 μl of immobilized GST resin (Novagen, Madison, WI) at 4 °C for 2 h and washed in PBS. Recombinant protein was eluted with a buffer containing 10 mM reduced glutathione.

Co-Immunoprecipitation

Co-immunoprecipitation and Western blotting were conducted as described previously [9, 43]. Briefly, ER microsomes (250 μg protein per sample) were prepared from adult mouse whole brains as described previously [9, 10, 46]. Samples were incubated alone, with RyR2 antibody (AB9080), or anti-rabbit IgG (2 mg/ml; Jackson Laboratories, Baltimore, PA) with or without recombinant calsenilin protein with a GST tag (combined molecular weight was between 51 and 55 kDa) under constant shaking at 4 °C for 12 h. Following incubation, samples were combined with protein A magnetic beads (EMD Millipore) for 10 min at RT, washed three times in PBS with 0.1% Tween 20, and eluted with Western Blot Sample Buffer (10%, glycerol: 10%, β-mercaptoethanol: 1%, bromophenol blue: 0.004%, tris (hydroxymethyl) aminomethane (Tris)-HCl: 0.5 M, pH 6.8) at 80 °C for 10 min.

Western Blotting

Solubilized proteins and molecular weight markers (HiMark™ Pre-stained Protein Standard, Thermo Fisher Scientific, Waltham, MA) were separated on a 3–8% NuPAGE® Novex® Midi Tris-acetate gel (Life Technologies) and transferred to Amersham Hybond-ECL blotting paper (0.45 μm, GE Healthcare). Blots were incubated for 12–16 h at 4 °C with the calsenilin antibody (05–756) (1:500; Upstate, Lake Placid) and a RyR2 antibody (MA3–916) (1:100; Thermo Fisher Scientific). Blots were incubated with a horseradish peroxidase (HRP)-linked secondary antibody (31430) (1:5000; Thermo Fisher Scientific) at RT for 1 h. Membranes were developed using SuperSignal West Femto Chemiluminescent Substrate (Thermo Fisher Scientific) and imaged on the Syngene G:BOX using Syngene GeneSnap acquisition software.

Single-Channel Electrophysiology

Electrophysiology was conducted as previously stated [21, 22, 36]. Microsomes were added to the *cis* compartment of the bilayer chamber (Warner Instruments, Hamden, CT), where they were fused to a lipid bilayer formed with a 3:1 mixture of dried phosphatidylethanolamine/phosphatidylserine lipids (Avanti Polar Lipids, Alabaster, AL) on a 150 μm diameter aperture using hyperosmotic conditions (KCl solution of ~ 300–500 mM).The microsome incorporation was monitored by the appearance of channel activity and followed by perfusion of the cis chambers with 10 volumes of *cis* (106 mM Tris–OH, 220 mM HEPES, pH 7.35, ~ 320 mOsm) buffer. RyR-

mediated single-channel currents were activated by addition of Ca^{2+} into the cis chamber at fixed levels with rationed amounts of $CaCl_2$/EGTA calculated using MaxChelator software (Stanford University). Recombinant calsenilin protein was added to the cis side of the chamber. The RyR blocker ruthenium red (10–25 μM) was routinely added at the end of the experiment to verify the identity of the RyRs. Experiments were performed at RT with single-channel currents recorded at a holding potential of 0 mV (*trans* chamber grounded) using a BC-525 amplifier (Warner Instruments), filtered at 500 Hz and digitized at 5 kHz using pCLAMP™10 software (Molecular Devices, Sunnyvale, CA). pCLAMP™10 was used to conduct offline current trace filtering (320 Hz), to determine dwell time, to provide a amplitude histogram, and to calculate open-channel probability.

Single-Channel Electrophysiology Statistics

All recordings were normalized to control values and reported as percentage of controls. GraphPad Prism 5 (*GraphPad Software*, Inc., San Diego, CA) was used for all analysis and data presentation. Nonlinear curve fitting was performed using the Levenberg–Marquardt algorithm and tested for goodness of fit using the chi-squared algorithm. A one-way ANOVA with a Dunnett's post-hoc test was used to determine significance (Mean ± SEM; $p < 0.05$, *, $p < 0.01$, **, $p < 0.001$, ***).

Transfection

Calsenilin cDNA was prepared from total RNA using SuperScript™ (Invitrogen) II Reverse Transcriptase (RT) (Thermo Fisher Scientific) and poly T primers, as described previously [9]. SH-SY5Y neuroblastoma cells (ATCC, Manassas, VA) were co-transfected per manufacturer's instruction using a Lonza 4D-nucleofector transfection unit (Lonza, Walkersville, MD). Briefly, cells were suspended in Lonza transfection media with 2 μg of calsenilin pcDNA3.1 (+) Zeo mammalian expression vector and 0.5 μg of tdTomato (reporter protein) pcDNA3.1 (+) Zeo mammalian expression vector. Transfected cells were then plated at 25000 cells per laminin/poly-d lysine coverslips (BD Biocoat, Bedford, MA) using SH-SY5Y media (10% fetal bovine serum (PAA, Piscataway, NJ)), 1:200 penicillin/streptomycin, 50% Ham's F-12 media, and 50% Eagle's minimum essential media (Lonza, Walkersville, MD) and maintained at 37 °C, 5% CO_2, and 95% O_2 for 36–48 h.

Calcium Imaging

Media from mock- or calsenilin-transfected SH-SY5Y cells were removed and washed in extracellular solution buffer (ECS) (137 mM NaCl, 5 mM KCl, 1 mM Na_2HPO_4, 1 mM $MgSO_4$, 10 mM HEPES, 22 mM D-(+)-glucose, and 1.8 mM $CaCl_2$; pH 7.35 at 37 °C); then, cells were incubated in 2 μM fura-2 AM (Invitrogen) in ECS for 30 min. Coverslips were washed with ECS containing 55 mM KCl to empty and subsequently refill their intracellular Ca^{2+} stores; they were then washed two more times with ECS. Coverslips were assembled to the imaging platform and continually perfused at 2 ml/min with ECS at a constant temperature of 37 °C. Perfusion protocols were the same for all experiments and controlled through MetaFluor sequential journals. The perfusion protocol was as follows: 1 min of ECS to establish a baseline, 3 min of 30 mM caffeine in ECS to stimulate the RyRs, and 3 min of ECS to return the response to baseline. Regions of interests (ROIs) were selected following Ca^{2+} imaging to adjust for drift. Background ROIs ($N = 4$ for each coverslip) were selected using a region of the optical field not occupied by cells.

Calcium Imaging Statistical Analysis

GraphPad Prism 5 was used for all analysis and data presentation. The calculation for the area under the curve (AUC) was defined as follows: the beginning of the curve was the time point where the Ca^{2+} value rose above 5% of baseline, and the ending of the curve was defined by the last point in the curve that was above 5% of the baseline. Both maximum value and width of response were calculated from this curve. Linear regression was done to calculate the slope values of each response using the max value and the first point 5% above the baseline. All values were averaged and statistically analyzed using Student's *t* test (Mean ± SEM; $p < 0.05$, *; $p < 0.01$, **; $p < 0.001$, ***).

Results

Calsenilin and RyR Are Co-localized and Have a Direct Protein-Protein Interaction in Neuronal Tissue

Figure 1 shows typical calsenilin and RyR2 or RyR3 (Fig. 1a) staining patterns in primary cultured cortical neurons and RyR2 in the dentate gyrus and cortical layer VI of a 6-week-old C57 mouse brain (Fig. 1b). Colocalization between the two proteins is highest in the perinuclear region of the cells for both RyR2 and RyR3. This staining pattern is indicative of ER Ca^{2+} release channels in neuronal tissue [47–49]. Figure 1c shows this pattern of colocalization, which appears for RyR2 and calsenilin in all cortical neurons and hippocampal and cortical layers tested. Colocalization of RyR3 and calsenilin in both the hippocampus and the cortex is region-specific with higher co-localization seen in the CA3 region of the hippocampus and cortical layer VI (Fig. 1c). Immunoblotting of proteins captured using an anti-RyR2 antibody (Fig. 1d) shows expression of both RyR2 (approximately 550 kDa) and calsenilin recombinant protein with a

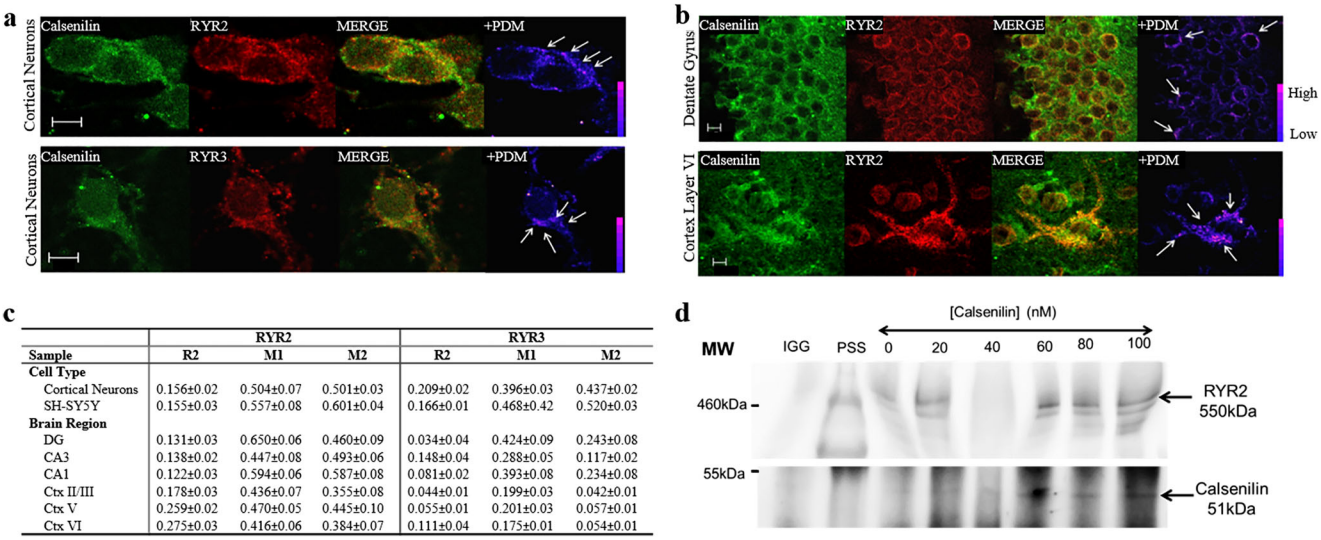

c

	RYR2			RYR3		
Sample	**R2**	**M1**	**M2**	**R2**	**M1**	**M2**
Cell Type						
Cortical Neurons	0.156±0.02	0.504±0.07	0.501±0.03	0.209±0.02	0.396±0.03	0.437±0.02
SH-SY5Y	0.155±0.03	0.557±0.08	0.601±0.04	0.166±0.01	0.468±0.42	0.520±0.03
Brain Region						
DG	0.131±0.03	0.650±0.06	0.460±0.09	0.034±0.04	0.424±0.09	0.243±0.08
CA3	0.138±0.02	0.447±0.08	0.493±0.06	0.148±0.04	0.288±0.05	0.117±0.02
CA1	0.122±0.03	0.594±0.06	0.587±0.08	0.081±0.02	0.393±0.08	0.234±0.08
Ctx II/III	0.178±0.03	0.436±0.07	0.355±0.08	0.044±0.01	0.199±0.03	0.042±0.01
Ctx V	0.259±0.02	0.470±0.05	0.445±0.10	0.055±0.01	0.201±0.03	0.057±0.01
Ctx VI	0.275±0.03	0.416±0.06	0.384±0.07	0.111±0.04	0.175±0.01	0.054±0.01

Fig. 1 Calsenilin and RyR are co-localized and have a direct protein-protein interaction in neuronal tissue. Calsenilin (green) and **a** RyR2 or RyR3 (red) immunoreactivity in E18 primary cultured cortical neurons. **b** RyR2 (red) expression in the dentate gyrus and cortical layer VI shows a perinuclear staining pattern in regions adjacent to the nucleus indicative of ER staining (Merge) and a high degree of punctate colocalization in the perinuclear region (+PDM) as indicated by arrows and LUT in the last panel. **c** Colocalization measurements between calsenilin and RyR2 or RyR3 for neuronal cell types (E18 primary cortical neurons and SH-SY5Y neuroblastoma cells) and 6-week-old C57BL/6 mouse brain sections (dentate gyrus, CA3, CA1, cortical layers II/III, V, VI). The Rr = Pearson's coefficient and M1 = Mander's coefficient describe the amount of calsenilin co-localized with the two RyR subtypes, whereas the M2 = Mander's coefficient describes the amount of RyR2 or RyR3 co-localized with calsenilin. Statistical significance represents the SEM for each replicate; co-localization was tested with the Costes method to ensure true co-localization. **d** Western blot shows the presence of calsenilin in the brain-derived ER microsomes incubated with calsenilin protein and subjected to co-immunoprecipitation separation using the RyR2 antibody; the IgG control is shown in lane "IgG," and molecular weight standards are shown in lane "PSS." Abbreviations: RyR, ryanodine receptor; DG, dentate gyrus; CA1 or CA3, Cornu Ammonis 1 or 3; Ctx, cortex layer; IgG, immunoglobulin G; MW, molecular weight; PSS, pre-stained standard

GST tag (approximately 51 kDa). Substituting the anti-RyR2 antibody with IgG yielded no bands for RyR2 or calsenilin (Fig. 1d), proving the specificity of the anti-RyR2 antibody. Together these data suggest that calsenilin and RyR2/RyR3 not only reside in the same subcellular location, but interact.

Calsenilin Alters RyR Single-Channel Ca^{2+} Release in Single-Channel Electrophysiological Experiments

Figure 2 shows typical recordings of RyR activity at physiological intracellular calcium ion concentrations of 100 nM (pCa7; Fig. 2a), 1 μM (pCa6; Fig. 2c), and 10 μM (pCa5; Fig. 2e) before and after calsenilin addition. The pCa7 amplitude histogram (Fig. 2b) shows that calsenilin reduces the number of times the channel opens and decreases the duration of each opening. The decrease in the number and duration of channel openings translates to a significant decrease in the open probability of the subconductance state (−2 pA) of the RyR (Fig. 2g). This data suggests that at a resting cytosolic Ca^{2+} concentration, calsenilin decreases Ca^{2+} release from RyRs. Conversely, at higher Ca^{2+} concentrations, calsenilin has the opposite effect on RyR single-channel kinetics. After the addition of calsenilin (Fig. 2c, d), RyR activity increases, characterized by an increase in the number of times the channel opens and the duration of each opening (Fig. 2d). The changes in RyR activity after the addition of calsenilin at 1 μM Ca^{2+} translate to a significant increase in the open probability of the channel at the subconductance (−2 pA; Fig. 2g) and full conductance state (−4 pA; Fig. 2h). Similarly, the activity of the RyR at 10 μM Ca^{2+} after the addition of calsenilin shows increases in frequency and duration of openings (Fig. 2e–h), translating into a significant increase of the full conductance state (−4 pA; Fig. 2h). At 100 μM Ca^{2+}, the addition of calsenilin did not result in significantly different RyR channel activity (data not shown). The data indicates that calsenilin affects the Ca^{2+} release kinetics of the RyR in a Ca^{2+} concentration-dependent fashion. Calsenilin causes a sharpening of the CICR of RyRs by significantly decreasing the activity of the receptor in a normally low-activity state (100 nM Ca^{2+}) and increasing receptor activity at high activity states (1 and 10 μM, respectively).

Calsenilin Overexpression in SH-SY5Y Neuroblastoma Cells Alters Caffeine-Induced Ca^{2+} Release

Figure 3 shows a typical caffeine-induced Ca^{2+} response in SH-SY5Y control cells (black line) and calsenilin overexpressing cells (red line). Calsenilin overexpression increases the release rate of Ca^{2+} from RyR-sensitive stores compared to control cells.

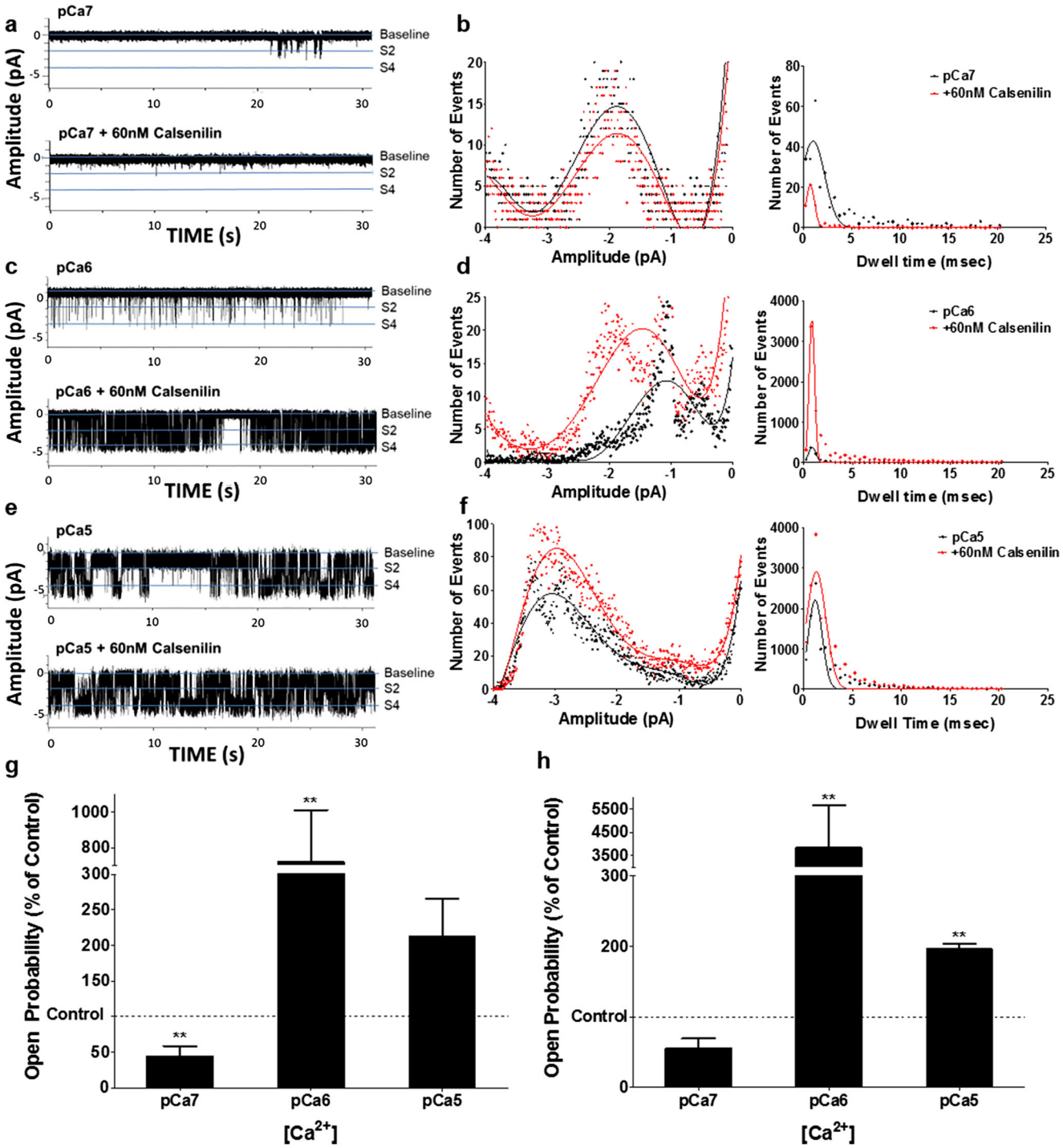

Fig. 2 Calsenilin causes calcium concentration-dependent alterations in the biophysical Ca^{2+} release from single brain RyRs. Representative planar lipid bilayer 60 s traces (**a**, **c**, and **e**) at varying physiological calcium concentrations in the presence (bottom trace) and absence (top trace) of calsenilin, and respective histograms (**b**, **d**, and **f**) for amplitude (pA, left) and dwell time (msec, right). Graphs G and H show the open probability of the RyR in the presence of 60 nM calsenilin for $i_o = -2$ pA and -4 pA, respectively, expressed as the percentage of the respective controls recorded in the absence of calsenilin at pCa4–7 (one-way ANOVA with Dunnett's post-test; values are represented as mean ± SEM; ***, $p < 0.001$ and **, $p < 0.01$; $n = 3$–8).

Calculation of the slope of Ca^{2+} release for both control and calsenilin overexpressing cells shows a significant increase in the rate of Ca^{2+} release (Fig. 3b). The increased calcium release rate corresponds to a significant decrease in the duration of Ca^{2+} release of calsenilin overexpressing cells as compared to control cells calculated by the width of Ca^{2+} release (Fig. 3d). The maximum amplitude of caffeine-induced Ca^{2+} release is significantly increased in calsenilin overexpressing cells compared to control

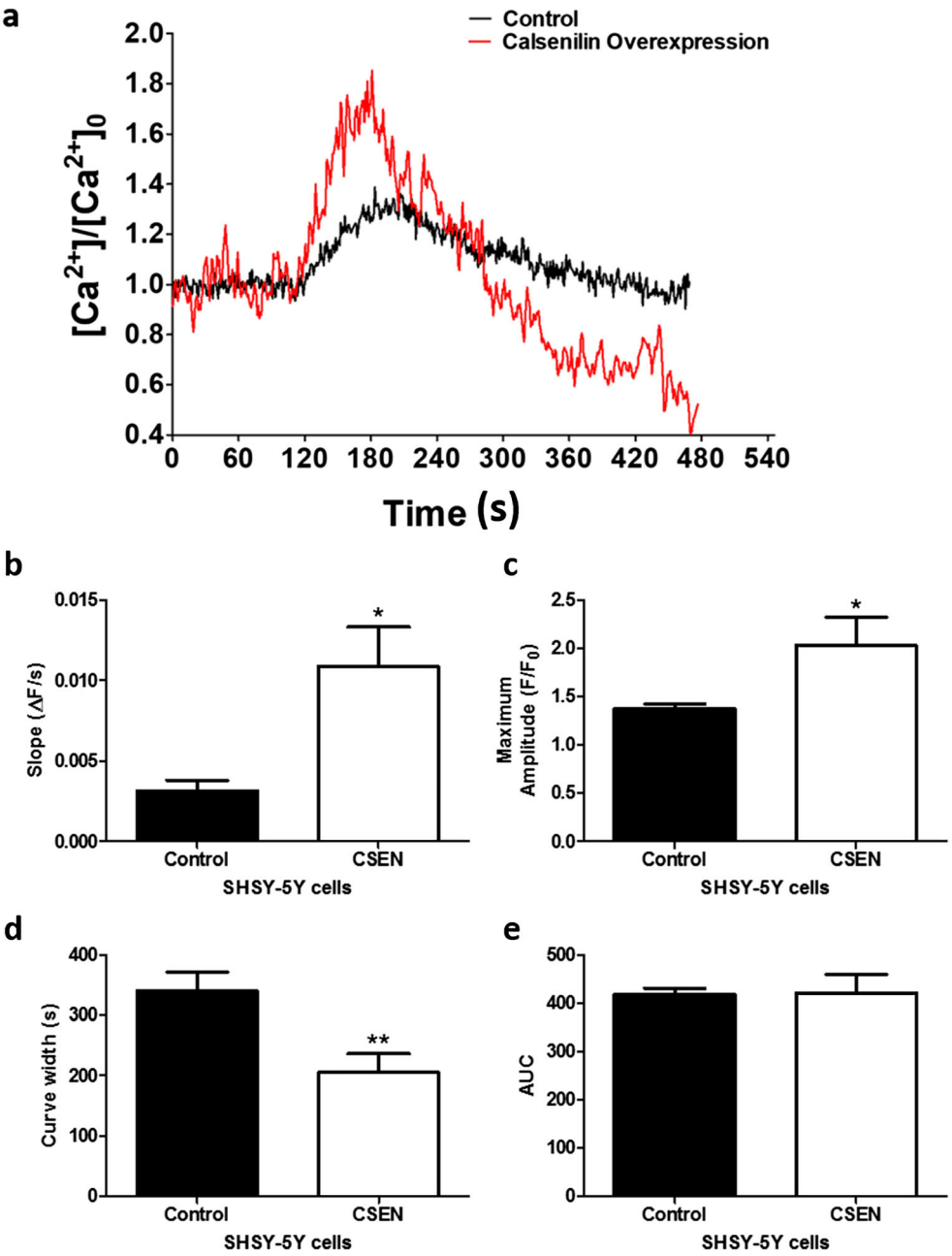

Fig. 3 Calsenilin changed the kinetics of caffeine-induced calcium release. Representative traces showing caffeine-induced calcium release from untransfected (black trace) and calsenilin-transfected (red trace) SH-SY5Y cells (**a**), and the respective kinetic analysis of slope (**b**), maximum amplitude (**c**), duration (**d**), and area under the curve (**e**) (Student's *t* test; values represented as mean ± SEM; *, $p < 0.05$; **, $p < 0.01$; $n = 3–8$).

cells (Fig. 3c). Interestingly, a calculation of the area under the curve, which is a relative measure of the amount of Ca^{2+} released, shows no difference between control cells and calsenilin overexpressing cells (Fig. 3e). Together these data suggest that calsenilin modulates CICR kinetics of the RyR.

Discussion

We have shown that calsenilin and RyR2 and RyR3 co-localize in the endoplasmic reticulum of mouse hippocampal and cortical neurons (Fig. 1a–c) and have a probable protein-protein interaction between calsenilin and RyR2 in microsomes derived from brain tissue (Fig. 1d). We found that calsenilin causes calcium ion concentration-dependent alterations in the Ca^{2+} release from single brain RyRs (Fig. 2) and alters the kinetics of caffeine-induced calcium release from intracellular stores in a whole cell paradigm (Fig. 3). The modulation of single-channel RyRs by calsenilin decreased channel activity at lower 100-nM calcium concentrations (Fig. 2a, b, g, h) and increased channel activity at 1 and 10 μM calcium concentrations (Fig. 2c–f, g, h). In a whole cell paradigm, calsenilin modulation of multiple RyRs caused faster and higher amplitude caffeine-induced calcium release

in SH-SY5Y cells overexpressing calsenilin (Fig. 3). The alteration in calcium release dynamics from RyRs can have profound effects on the functioning of neurons.

Transient increases in calcium concentration in neurons can lead to opposite responses based on magnitude, timing, and duration of the elevated calcium release. For example, the consolidation, or lack of consolidation, of memories through long-term potentiation (LTP) and long-term depression (LTD) is a function of firing patterns in pre- and post-synaptic neurons [50]. The magnitude and timing of calcium signals in neurites decide whether a signal received by a post-synaptic neuron will lead to LTP or LTD. LTP is a function of large rapid calcium transients, while LTD is a function of slow longer duration calcium transients [51]. These two phenomena are profoundly affected by release from intracellular calcium stores such as the RyRs and inositol triphosphate receptors (IP3Rs) [52]. Further, neuronal calcium sensors that affect the magnitude of calcium signals in neurons can change the polarization of growth cones, branching of neurites, and rate of elongation [51]. The novel interaction between calsenilin and RyRs describes a modulatory mechanism that can alter duration, timing, and magnitude of calcium transients in neurons.

Alterations in calcium-induced calcium signaling in neurons are implicated in several neurodegenerative diseases (Parkinson's disease [17]; multiple sclerosis [18]; neuroinflammation [19]; Huntington's disease [20]; reviewed in [53]). The long-standing calcium hypothesis of AD states that alterations in calcium homeostasis occur before the clinical symptoms of AD, but lead to the slow progressive decline of memory and cognition in sporadic AD (reviewed in [54]). Further, altered RyR calcium release in the dendrites of presymptomatic 3xTg-AD mice [55] and young AD mice [56] shows RyR-mediated release affects synaptic plasticity in hippocampal and cortical neurons. Calsenilin is expressed in hippocampal and cortical dendrites and is involved in synaptic plasticity [31–33]. Mellström et al. found dendritic changes in the hippocampal neurons of a transgenic mouse model expressing the daDREAM mutant, suggesting calsenilin is involved in structural plasticity in the hippocampus [32]. In the present study, we have shown that calsenilin and RyR2 have a high degree of colocalization in proximal dendritic branch points (Fig. 1b) indicating that this association occurs in more distal dendritic branches. Dysregulation of calcium homeostasis leads to an increase in resting calcium concentrations seen in both the soma [57] and dendrites [58] of neurons affected by AD, as well as in neurons of in vivo models of neuroinflammation [19] and Huntington's disease [20]. The association of calsenilin with RyRs increases calcium release at higher calcium levels and leads to faster and higher amplitude calcium transients in cells overexpressing calsenilin. The increase in calsenilin [59] and RyR [60] expression in AD, as well as increased resting calcium concentration in AD [57, 58], in vivo models of neuroinflammation [19], and Huntington's disease [20] taken together with the increase in RyR activity in the presence of calsenilin and high calcium concentrations indicates a role for this interaction in the etiology of AD and potentially other neurodegenerative diseases, such as Parkinson's disease [17], multiple sclerosis [18], neuroinflammation [19], and Huntington's disease [20].

From this data, we propose that calsenilin has an important modulatory role in calcium release from RyRs by which calsenilin acts as a filter on calcium-induced calcium release. By silencing the receptor at low physiological calcium concentrations and increasing the activity at higher physiological calcium concentrations, calsenilin sharpens calcium release from RyRs mimicking ion signals seen in neuronal cells. This novel interaction could be exploited pharmacologically to reduce calcium levels in neurodegenerative disorders by displacing calsenilin from the RyR. The exact binding sites and calcium dependence of this interaction must be explored to further utilize this potential tool for the alleviation of neuronal dysfunction in neurodegeneration.

Acknowledgements Research reported in this publication was supported in part by grants from the National Eye Institute (EY014227 and EY022774), the Institute on Aging (AG022550 and AG027956), the National Center for Research Resources, and National Institute of General Medical Sciences (RR027093) of the National Institutes of Health (PK). The content is solely the responsibility of the authors and does not necessarily represent the official views of the National Institutes of Health. Additional support by the Felix and Carmen Sabates Missouri Endowed Chair in Vision Research and a Challenge Grant from Research to Prevent Blindness (PK) is gratefully acknowledged.

References

1. Berridge MJ, Bootman MD, Roderick HL (2003) Calcium signalling: dynamics, homeostasis and remodelling. Nat Rev Mol Cell Biol 4:517–529
2. Giannini G, Conti A, Mammarella S, Scrobogna M, Sorrentino V (1995) The ryanodine receptor/calcium channel genes are widely and differentially expressed in murine brain and peripheral tissues. J Cell Biol 128:893–904
3. Lanner JT, Georgiou DK, Joshi AD, Hamilton SL (2010) Ryanodine receptors: structure, expression, molecular details, and function in calcium release. Cold Spring Harb Perspect Biol 2: a003996
4. Weiss JL, Hui H, Burgoyne RD (2010) Neuronal calcium sensor-1 regulation of calcium channels, secretion, and neuronal outgrowth. Cell Mol Neurobiol 30:1283–1292
5. Johenning FW, Zochowski M, Conway SJ, Holmes AB, Koulen P, Ehrlich BE (2002) Distinct intracellular calcium transients in neurites and somata integrate neuronal signals. J Neurosci 22: 5344–5353
6. Hakamata Y, Nakai J, Takeshima H, Imoto K (1992) Primary structure and distribution of a novel ryanodine receptor/calcium release channel from rabbit brain. FEBS Lett 312:229–235
7. Lai FA, Dent M, Wickenden C, Xu L, Kumari G, Misra M, Lee HB, Sar M et al (1992) Expression of a cardiac Ca(2+)-release channel isoform in mammalian brain. Biochem J 288(Pt 2):553–564

8. Van Petegem F (2012) Ryanodine receptors: structure and function. J Biol Chem 287:31624–31632
9. Rybalchenko V, Hwang SY, Rybalchenko N, Koulen P (2008) The cytosolic N-terminus of presenilin-1 potentiates mouse ryanodine receptor single channel activity. Int J Biochem Cell Biol 40:84–97
10. Hayrapetyan V, Rybalchenko V, Rybalchenko N, Koulen P (2008) The N-terminus of presenilin-2 increases single channel activity of brain ryanodine receptors through direct protein-protein interaction. Cell Calcium 44:507–518
11. Smith IF, Hitt B, Green KN, Oddo S, LaFerla FM (2005) Enhanced caffeine-induced Ca2+ release in the 3xTg-AD mouse model of Alzheimer's disease. J Neurochem 94:1711–1718
12. Kelliher M, Fastbom J, Cowburn RF, Bonkale W, Ohm TG, Ravid R, Sorrentino V, O'Neill C (1999) Alterations in the ryanodine receptor calcium release channel correlate with Alzheimer's disease neurofibrillary and beta-amyloid pathologies. Neuroscience 92: 499–513
13. Stutzmann GE et al (2007) Enhanced ryanodine-mediated calcium release in mutant PS1-expressing Alzheimer's mouse models. Ann N Y Acad Sci 1097:265–277
14. Chan SL, Mayne M, Holden CP, Geiger JD, Mattson MP (2000) Presenilin-1 mutations increase levels of ryanodine receptors and calcium release in PC12 cells and cortical neurons. J Biol Chem 275:18195–18200
15. Lee SY, Hwang DY, Kim YK, Lee JW, Shin IC, Oh KW, Lee MK, Lim JS et al (2006) PS2 mutation increases neuronal cell vulnerability to neurotoxicants through activation of caspase-3 by enhancing of ryanodine receptor-mediated calcium release. FASEB J 20: 151–153
16. Ferreiro E, Resende R, Costa R, Oliveira CR, Pereira CM (2006) An endoplasmic-reticulum-specific apoptotic pathway is involved in prion and amyloid-beta peptides neurotoxicity. Neurobiol Dis 23: 669–678
17. Huang L, Xue Y, Feng D, Yang R, Nie T, Zhu G, Tao K, Gao G et al (2017) Blockade of RyRs in the ER attenuates 6-OHDA-induced calcium overload, cellular hypo-excitability and apoptosis in dopaminergic neurons. Front Cell Neurosci 11:52. https://doi.org/10.3389/fncel.2017.00052.eCollection2017.
18. Ruiz A, Matute C, Alberdi E (2010) Intracellular Ca2+ release through ryanodine receptors contributes to AMPA receptor-mediated mitochondrial dysfunction and ER stress in oligodendrocytes. Cell Death Dis 1:e54. https://doi.org/10.1038/cddis.2010.31
19. Hopp SC, Royer SE, D'Angelo M, Kaercher RM, Fisher DA, Wenk GL (2015) Differential neuroprotective and anti-inflammatory effects of L-type voltage dependent calcium channel and ryanodine receptor antagonists in the substantia nigra and locus coeruleus. J NeuroImmune Pharmacol 10(1):35–44. https://doi.org/10.1007/s11481-014-9568-7
20. Raymond LA (2017) Striatal synaptic dysfunction and altered calcium regulation in Huntington disease. Biochem Biophys Res Commun 483(4):1051–1062. https://doi.org/10.1016/j.bbrc.2016.07.058
21. Burgoyne RD, Weiss JL (2001) The neuronal calcium sensor family of Ca2+-binding proteins. Biochem J 353:1–12
22. An WF, Bowlby MR, Betty M, Cao J, Ling HP, Mendoza G, Hinson JW, Mattsson KI et al (2000) Modulation of A-type potassium channels by a family of calcium sensors. Nature 403:553–556
23. Buxbaum JD, Choi EK, Luo Y, Lilliehook C, Crowley AC, Merriam DE, Wasco W (1998) Calsenilin: a calcium-binding protein that interacts with the presenilins and regulates the levels of a presenilin fragment. Nat Med 4:1177–1181
24. Carrion AM, Link WA, Ledo F, Mellstrom B, Naranjo JR (1999) DREAM is a Ca2+-regulated transcriptional repressor. Nature 398: 80–84
25. Buxbaum JD, Lilliehook C, Chan JY, Go RCP, Bassett SS, Tanzi RE, Wasco W, Blacker D (2000) Genomic structure, expression pattern, and chromosomal localization of the human calsenilin gene: no association between an exonic polymorphism and Alzheimer's disease. Neurosci Lett 294:135–138
26. Zaidi NF, Berezovska O, Choi EK, Miller JS, Chan H, Lilliehook C, Hyman BT, Buxbaum JD et al (2002) Biochemical and immunocytochemical characterization of calsenilin in mouse brain. Neuroscience 114:247–263
27. Duncan CE, Schofield PR, Weickert CS (2009) K(v) channel interacting protein 3 expression and regulation by haloperidol in midbrain dopaminergic neurons. Brain Res 1304:1–13
28. Hammond PI, Craig TA, Kumar R, Brimijoin S (2003) Regional and cellular distribution of DREAM in adult rat brain consistent with multiple sensory processing roles. Brain Res Mol Brain Res 111:104–110
29. Spreafico F, Barski JJ, Farina C, Meyer M (2001) Mouse DREAM/calsenilin/KChIP3: gene structure, coding potential, and expression. Mol Cell Neurosci 17:1–16
30. Wang WC, Cheng CF, Tsaur ML (2015) Immunohistochemical localization of DPP10 in rat brain supports the existence of a Kv4/KChIP/DPPL ternary complex in neurons. J Comp Neurol 523:608–628
31. Johnston D, Christie BR, Frick A, Gray R, Hoffman DA, Schexnayder LK, Watanabe S, Yuan LL (2003) Active dendrites, potassium channels and synaptic plasticity. Philos Trans R Soc Lond Ser B Biol Sci 358:667–674
32. Mellström B, Kastanauskaite A, Knafo S, Gonzalez P, Dopazo XM, Ruiz-Nuño A, Jefferys JGR, Zhuo M et al (2016) Specific cytoarchitectureal changes in hippocampal subareas in daDREAM mice. Mol Brain 9:22
33. Sanchez-Aguilera A, Sanchez-Alonso JL, Vicente-Torres MA, Colino A (2014) A novel short-term plasticity of intrinsic excitability in the hippocampal CA1 pyramidal cells. J Physiol 592:2845–2864
34. Cheng CF, Wang WC, Huang CY, du PH, Yang JH, Tsaur ML (2016) Coexpression of auxiliary subunits KChIP and DPPL in potassium channel Kv4-positive nociceptors and pain-modulating spinal interneurons. J Comp Neurol 524:846–873
35. Jo DG, Jang J, Kim BJ, Lundkvist J, Jung YK (2005) Overexpression of calsenilin enhances gamma-secretase activity. Neurosci Lett 378:59–64
36. Gomez-Villafuertes R, Torres B, Barrio J, Savignac M, Gabellini N, Rizzato F, Pintado B, Gutierrez-Adan A et al (2005) Downstream regulatory element antagonist modulator regulates Ca2+ homeostasis and viability in cerebellar neurons. J Neurosci 25:10822–10830
37. Leissring MA, Yamasaki TR, Wasco W, Buxbaum JD, Parker I, LaFerla FM (2000) Calsenilin reverses presenilin-mediated enhancement of calcium signaling. Proc Natl Acad Sci U S A 97: 8590–8593
38. Lilliehook C, Chan S, Choi EK, Zaidi NF, Wasco W, Mattson MP, Buxbaum JD (2002) Calsenilin enhances apoptosis by altering endoplasmic reticulum calcium signaling. Mol Cell Neurosci 19:552–559
39. Fedrizzi L, Lim D, Carafoli E, Brini M (2008) Interplay of the Ca2+-binding protein DREAM with presenilin in neuronal Ca2+ signaling. J Biol Chem 283:27494–27503
40. Jo DG et al (2001) Pro-apoptotic function of calsenilin/DREAM/KChIP3. FASEB J 15:589–591
41. Jo DG, Lee JY, Hong YM, Song S, Mook-Jung I, Koh JY, Jung YK (2004) Induction of pro-apoptotic calsenilin/DREAM/KChIP3 in Alzheimer's disease and cultured neurons after amyloid-beta exposure. J Neurochem 88:604–611
42. Rybalchenko V, Grillo MA, Gastinger MJ, Rybalchenko N, Payne AJ, Koulen P (2009) The unliganded long isoform of estrogen receptor beta stimulates brain ryanodine receptor single channel

activity alongside with cytosolic Ca2+. J Recept Signal Transduct Res 29:326–341
43. Duncan RS, Hwang SY, Koulen P (2007) Differential inositol 1,4, 5-trisphosphate receptor signaling in a neuronal cell line. Int J Biochem Cell Biol 39:1852–1862
44. Beisker W, Dolbeare F, Gray JW (1987) An improved immunocytochemical procedure for high-sensitivity detection of incorporated bromodeoxyuridine. Cytometry 8:235–239
45. Collin T McMaster Biophotonics Facility, McMaster University, Hamilton
46. Hwang SY, Wei J, Westhoff JH, Duncan RS, Ozawa F, Volpe P, Inokuchi K, Koulen P (2003) Differential functional interaction of two Vesl/Homer protein isoforms with ryanodine receptor type 1: a novel mechanism for control of intracellular calcium signaling. Cell Calcium 34:177–184
47. Terasaki M, Slater NT, Fein A, Schmidek A, Reese TS (1994) Continuous network of endoplasmic reticulum in cerebellar Purkinje neurons. Proc Natl Acad Sci U S A 91:7510–7514
48. Sharp AH, McPherson P, Dawson TM, Aoki C, Campbell KP, Snyder SH (1993) Differential immunohistochemical localization of inositol 1,4,5-trisphosphate- and ryanodine-sensitive Ca2+ release channels in rat brain. J Neurosci 13:3051–3063
49. Seymour-Laurent KJ, Barish ME (1995) Inositol 1,4,5-trisphosphate and ryanodine receptor distributions and patterns of acetylcholine- and caffeine-induced calcium release in cultured mouse hippocampal neurons. J Neurosci 15:2592–2608
50. Feldman DE (2012) The spike-timing dependence of plasticity. Neuron 75:556–571
51. Burgoyne RD (2007) Neuronal calcium sensor proteins: generating diversity in neuronal Ca2+ signalling. Nat Rev Neurosci 8:182–193
52. Ross WN (2012) Understanding calcium waves and sparks in central neurons. Nat Rev Neurosci 13:157–168
53. Duncan RS, Goad DL, Grillo MA, Kaja S, Payne AJ, Koulen P (2010) Control of intracellular calcium signaling as a neuroprotective strategy. Molecules 15:1168–1195
54. Berridge MJ (2011) Calcium signalling and Alzheimer's disease. Neurochem Res 36:1149–1156
55. Chakroborty S, Goussakov I, Miller MB, Stutzmann GE (2009) Deviant ryanodine receptor-mediated calcium release resets synaptic homeostasis in presymptomatic 3xTg-AD mice. J Neurosci 29: 9458–9470
56. Goussakov I, Miller MB, Stutzmann GE (2010) NMDA-mediated Ca(2+) influx drives aberrant ryanodine receptor activation in dendrites of young Alzheimer's disease mice. J Neurosci 30:12128–12137
57. Lopez JR, Lyckman A, Oddo S, LaFerla FM, Querfurth HW, Shtifman A (2008) Increased intraneuronal resting [Ca2+] in adult Alzheimer's disease mice. J Neurochem 105:262–271
58. Kuchibhotla KV, Goldman ST, Lattarulo CR, Wu HY, Hyman BT, Bacskai BJ (2008) Abeta plaques lead to aberrant regulation of calcium homeostasis in vivo resulting in structural and functional disruption of neuronal networks. Neuron 59:214–225
59. Jin JK, Choi JK, Wasco W, Buxbaum JD, Kozlowski PB, Carp RI, Kim YS, Choi EK (2005) Expression of calsenilin in neurons and astrocytes in the Alzheimer's disease brain. Neuroreport 16:451–455
60. Supnet C, Grant J, Kong H, Westaway D, Mayne M (2006) Amyloid-beta-(1-42) increases ryanodine receptor-3 expression and function in neurons of TgCRND8 mice. J Biol Chem 281: 38440–38447